

# Development and Evaluation of RRTMG\_SW, a Shortwave Radiative Transfer Model for General Circulation Model Applications

*M. J. Iacono, J. S. Delamere, E. J. Mlawer, and S. A. Clough  
Atmospheric and Environmental Research, Inc.  
Lexington, Massachusetts*

*J.-J. Morcrette  
European Center for Medium-Range Weather Forecasts  
Reading, United Kingdom*

*Y.-T. Hou  
National Centers for Environmental Prediction  
Camp Springs, Maryland*

## Introduction

The k-distribution shortwave radiation model developed for the Atmospheric Radiation Measurement (ARM) Program, RRTM\_SW\_V2.4 (Clough et al. 2004), utilizes the discrete ordinates radiative transfer model, DISORT, for scattering calculations and 16 g-points in each of its 16 spectral bands. DISORT provides agreement with line-by-line flux calculations to within  $1 \text{ Wm}^{-2}$  for direct irradiance and  $2 \text{ Wm}^{-2}$  for diffuse irradiance, but it makes RRTM\_SW too computationally expensive for direct use in general circulation models. To extend our earlier work in the longwave to address the ARM objective of improving radiative transfer models in general circulation models (Iacono et al. 2000), a new version of RRTM\_SW has been developed. This model, RRTMG\_SW, provides improved computational performance by using a 2-stream method for radiative transfer and scattering and by applying an optimized and reduced set of 112 total g-points while retaining a high degree of accuracy relative to RRTM\_SW for a diverse set of atmospheric profiles. More information on these models can be found at 'rtweb.aer.com', and versions of both the longwave and shortwave RRTM that have been accelerated for general circulation model applications will be made available at that web site.

RRTMG\_SW is being tested for possible implementation in the European Center for Medium Range Weather Forecasts (ECMWF) weather forecast model and the National Centers for Environmental Prediction (NCEP) Global Forecast System (GFS) model, which have been using the accelerated longwave model (RRTMG\_LW) operationally since June 2000 and August 2003, respectively. Shortwave fluxes and heating rates from these two dynamical models are compared to RRTM. It is shown that the general circulation model shortwave models significantly underestimate clear-sky absorption and therefore overestimate downward surface fluxes at the surface.

## Clear-Sky Evaluation

For clear-sky, the accuracy of RRTMG\_SW is established by comparison to RRTM\_SW. The latter, has been shown to calculate irradiance to within  $2 \text{ W m}^{-2}$  of the data-validated, high-resolution, multiple scattering model, CHARTS (Moncet and Clough 1997). Figure 1, shows scatter plots of clear-sky flux and heating rate differences between RRTMG\_SW using a 2-stream algorithm with a reduced set of 112 g-points and RRTM\_SW using DISORT with 16-streams and 224 g-points. Calculations were made over 42 layers using the diverse set of 42 atmospheric profiles of Garand et al. (2001), and differences are plotted as a function of the RRTM\_SW calculation with DISORT. Upwelling flux

RRTMG\_SW 2-STREAM\_112 & 16-DISORT\_224, 820-50000  $\text{cm}^{-1}$

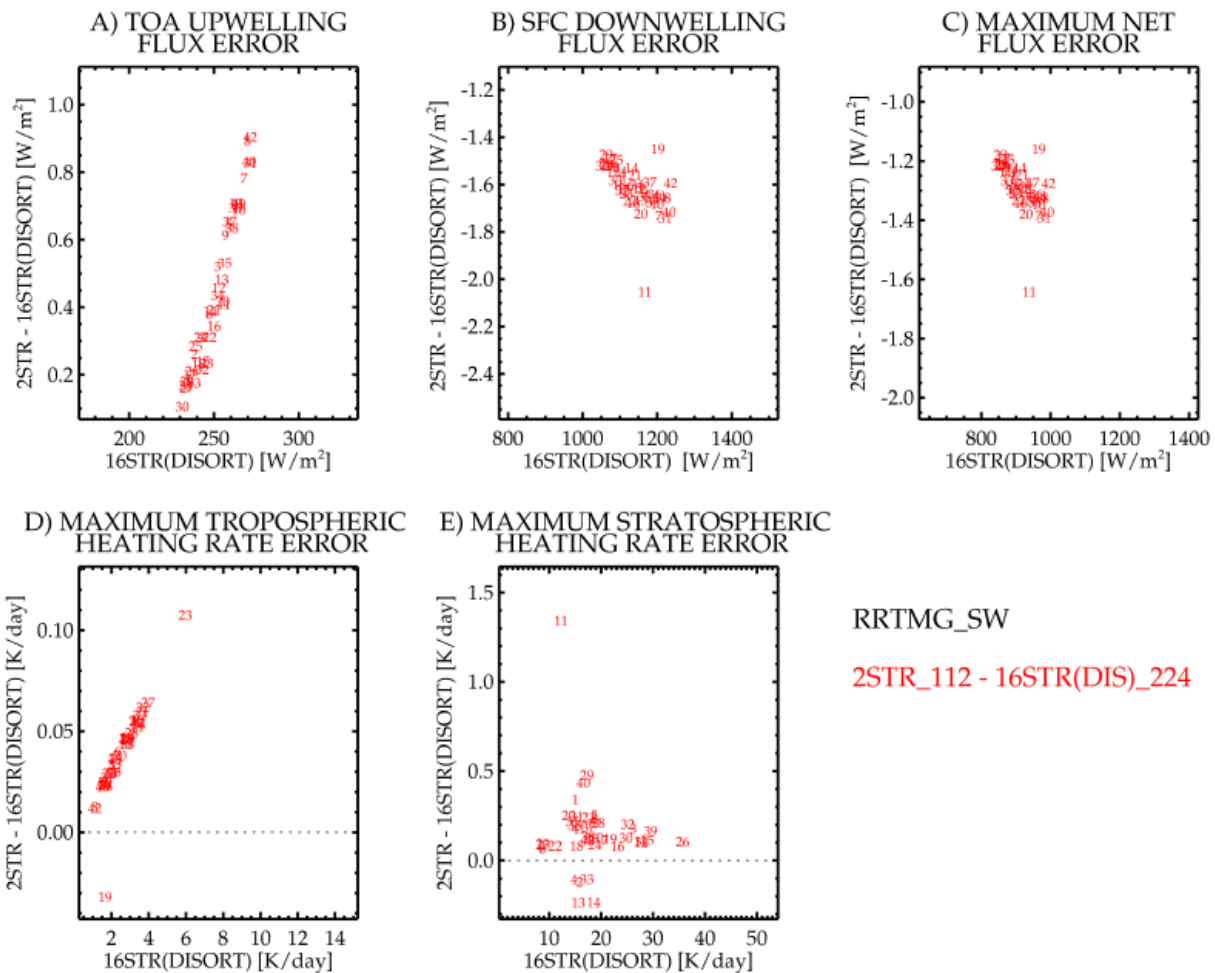


**Figure 1.** Scatter plots of clear-sky differences between RRTMG\_SW (using a 2-stream model) and RRTM\_SW (using DISORT) plotted as a function of the RRTM\_SW calculation for top of the atmosphere (TOA) upwelling flux (top left), surface downwelling flux (top middle), maximum net flux difference (top right), maximum tropospheric heating rate difference (bottom left), and maximum stratospheric heating rate difference (bottom right). Calculations are for the 42 diverse profiles of Garand et al. (2001), and values are plotted with a sequential number that identifies the profile.

differences at the TOA vary between 0.1 and 0.9  $\text{Wm}^{-2}$  depending on outgoing flux, while surface downwelling and maximum net flux differences cluster near 1.5  $\text{Wm}^{-2}$ . Maximum heating rate differences in the troposphere are only 0.05  $\text{Kd}^{-1}$ , while those in the stratosphere are generally less than 0.25  $\text{Kd}^{-1}$ . This demonstrates that selectively reducing the total number of g-points used by RRTMG\_SW to 112, which enhanced the model's computational performance by about a factor of two, had only small impacts on its accuracy.

## Evaluation with Low Cloud

A primary aspect of our model evaluation approach is to establish a link to measurements. The cloudy sky validation of spectral radiances from the CHARTS model with observations (Moncet and Clough, 1997) provides a basis for evaluating the broadband fluxes computed by RRTM\_SW and RRTMG\_SW. For a low cloud case using the tropical profile of Barker et al. (2002), a comparison between CHARTS and RRTM\_SW of upwelling and direct and diffuse downwelling fluxes has been previously documented (see Table 1 of Iacono et al. 2002). This case includes an overcast liquid cloud that consists of spherical droplets, is located in the layer from 3.5 to 4 km, has a mixing ratio of 0.159 g/kg, and has a visible optical depth close to 10. Both models use the liquid cloud parameterization of Hu and Stamnes (1993). For downwelling fluxes integrated over the 2600-50000  $\text{cm}^{-1}$  spectral region, RRTM\_SW agrees within 0.6  $\text{Wm}^{-2}$  of the fluxes calculated by CHARTS at the surface and at the top and bottom of the cloud. Upwelling diffuse flux differs by as much as 1.1  $\text{Wm}^{-2}$  at the cloud top.

Having shown the accuracy of the DISORT method used by RRTM\_SW, this model is utilized to evaluate the accuracy of the 2-stream approach used by RRTMG\_SW. For the same optically thick low cloud case described above, but applied to the Garand et al. (2001) profiles, Figure 2 shows scatter plots of flux and heating rate differences between these two models. Upwelling TOA flux, downward surface flux, and maximum net flux differences are about 1% and vary between 4 and 9  $\text{Wm}^{-2}$  depending on atmosphere. Maximum heating rate differences in the troposphere occur in the cloud layer and are about 1.4  $\text{Kd}^{-1}$ , or about 10%. The largest heating rate errors in the stratosphere are smaller and are consistent with the clear-sky case shown in Figure 1.

## RRTMG\_SW Comparison to NCEP\_SW

Having established the accuracy of the broadband models relative to the higher-resolution model, which has been validated with measurements, we can use RRTM\_SW/DISORT as a reference code to evaluate shortwave radiative transfer in general circulation models. Figure 3 shows a three-way, clear-sky 64-layer comparison between RRTM\_SW (in black), RRTMG\_SW (in red) and the NCEP shortwave code (in green) that is currently operational in the GFS medium-range forecast model. The upper three panels show shortwave heating rate differences, using RRTM\_SW as the reference, for the tropical, mid-latitude summer, and sub-arctic summer standard profiles. The two versions of RRTM produce nearly identical heating rates throughout the profiles, while NCEP\_SW produces too little heating through most of the atmosphere and especially in the stratospheric peak. The middle three panels of Figure 3 compare the TOA upwelling flux for the three models, while the bottom three panels show the downward surface fluxes. Significant flux differences between NCEP\_SW and both versions of RRTM are apparent that indicate too little clear-sky absorption in NCEP\_SW.

RRTMG\_SW 2-STREAM\_112 & 16-DISORT\_224, 820-50000 cm<sup>-1</sup>

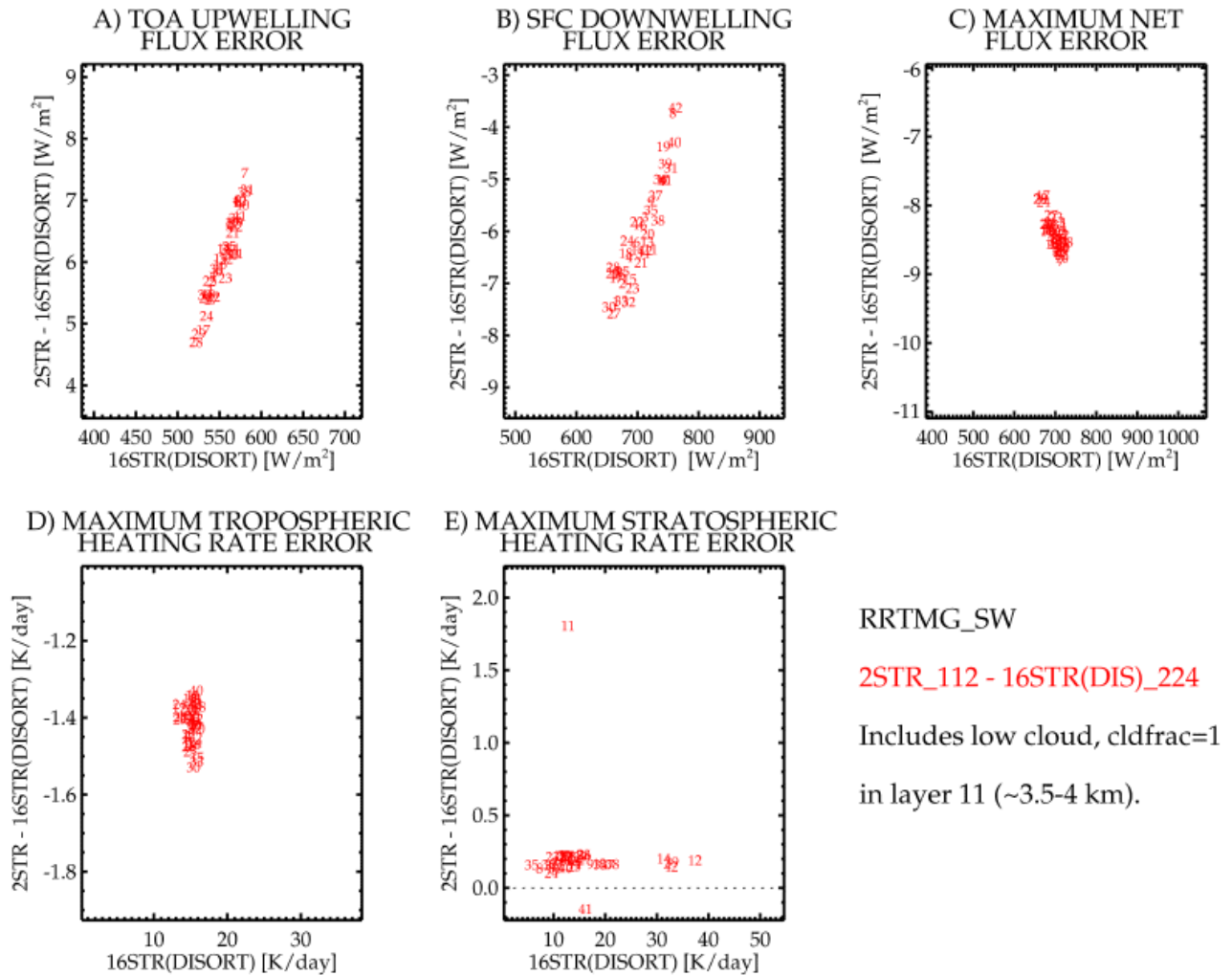


**Figure 2.** Scatter plots of cloudy sky differences between RRTMG\_SW (using a 2-stream model) and RRTM\_SW (using DISORT) plotted as a function of the RRTM\_SW calculation for TOA upwelling flux (top left), surface downwelling flux (top middle), maximum net flux difference (top right), maximum tropospheric heating rate difference (bottom left), and maximum stratospheric heating rate difference (bottom right). Calculations are for the 42 diverse profiles of Garand et al. (2001) with a single layer opaque low cloud, and values are plotted with a sequential number that identifies the profile.

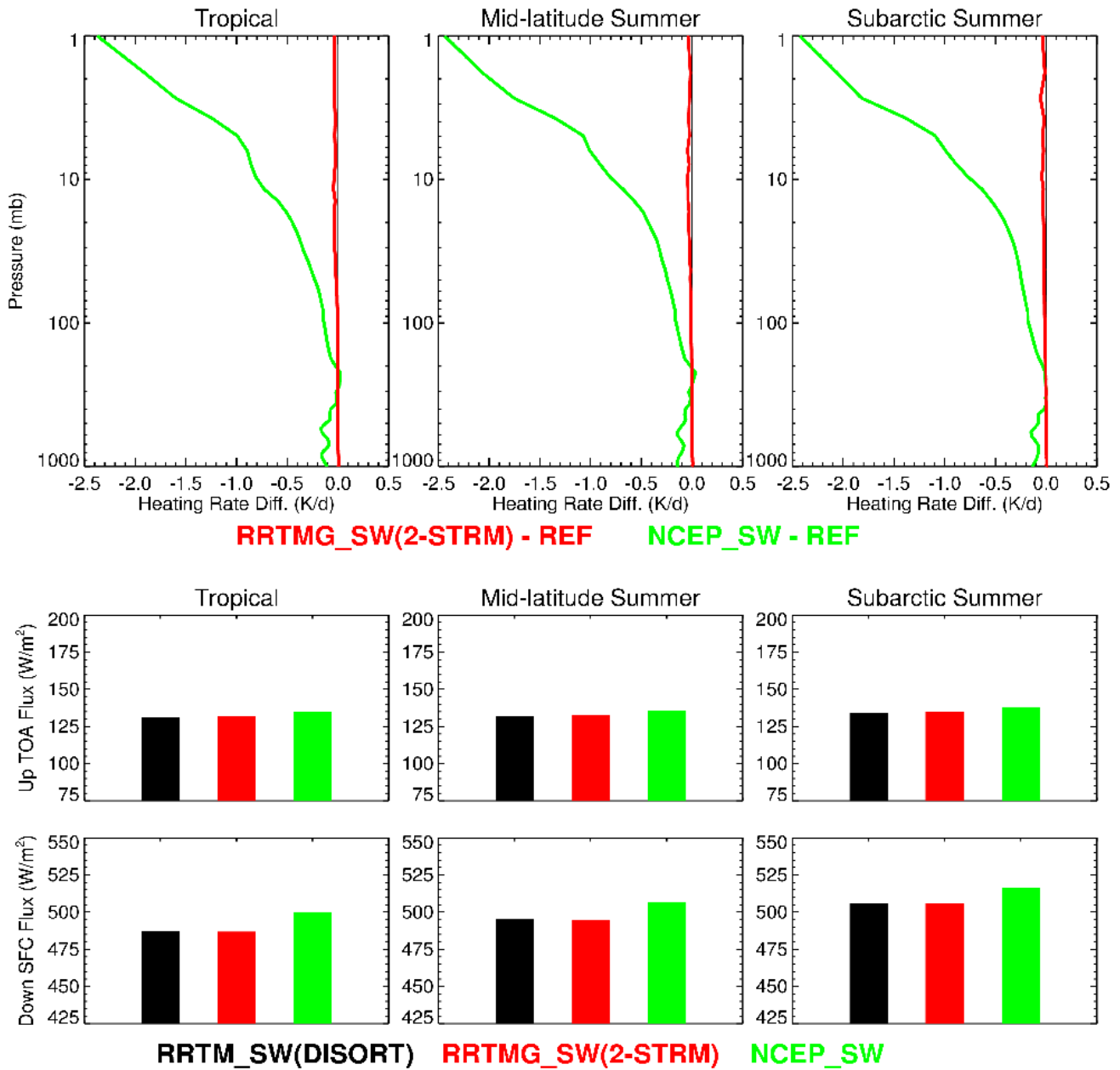


**Figure 3.** Clear-sky heating rate differences (top panels) between RRTMG\_SW and RRTM\_SW (red) and between NCEP\_SW and RRTM\_SW (green), clear-sky upward TOA fluxes for each model (middle panels), and downward surface fluxes (bottom panels), for the tropical, mid-latitude summer, and subarctic summer standard atmospheres.

Significant shortwave model differences are also apparent for the three standard atmospheres with two cloud layers. Figure 4 shows a comparison of heating rate and fluxes for the three shortwave models for 64-layer calculations including a high cloud near 350 mb with fraction 0.8 and a low cloud near 925 mb with fraction 0.4. Since the reference model, RRTM\_SW/DISORT, does not have partial cloud fraction capability, calculations for all models were performed for fully clear and fully overcast conditions. For

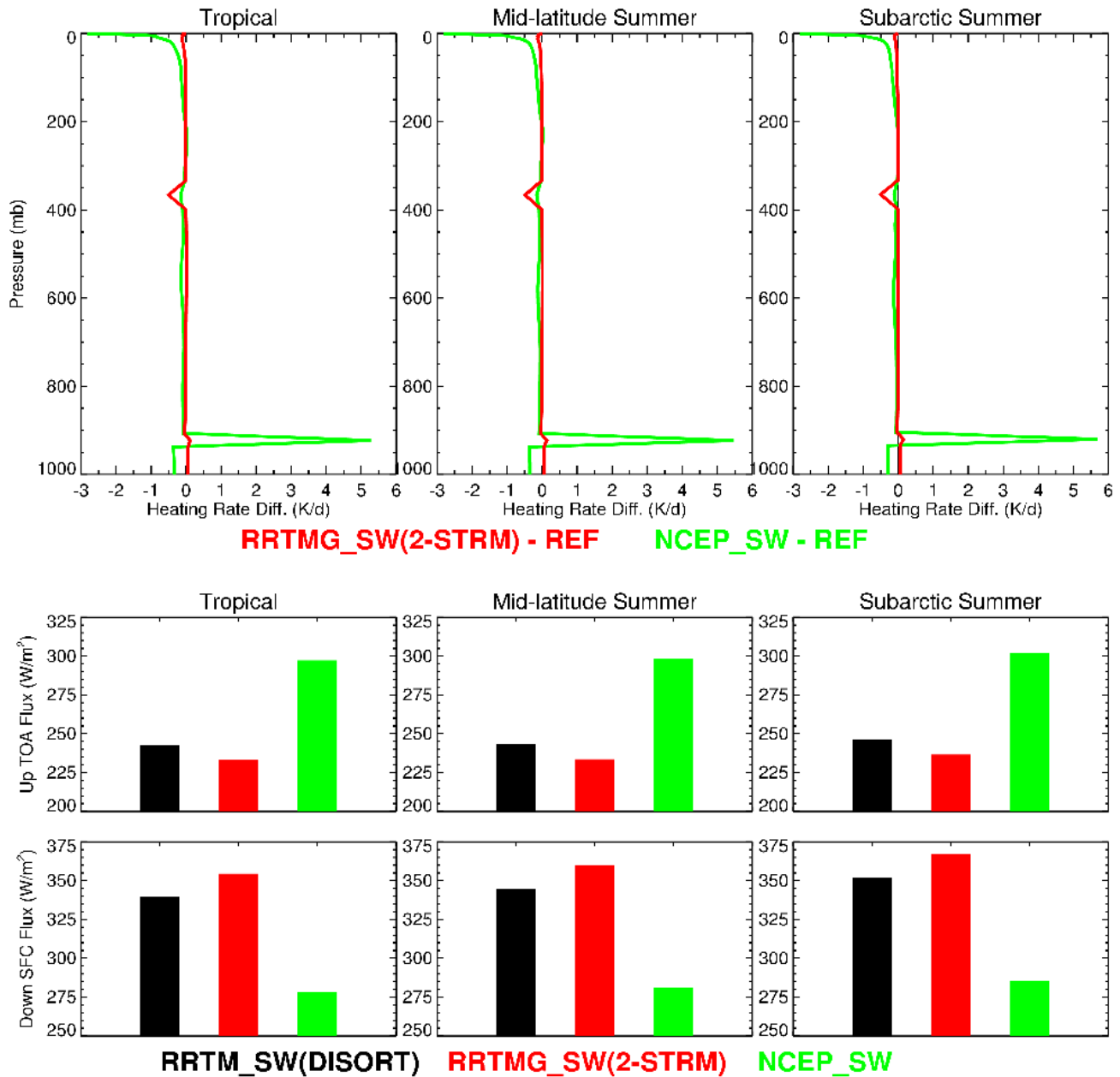


**Figure 4.** Cloudy sky heating rate differences (top panels) between RRTMG\_SW and RRTM\_SW (red) and between NCEP\_SW and RRTM\_SW (green), clear-sky upward TOA fluxes for each model (middle panels), and downward surface fluxes (bottom panels), for the tropical, mid-latitude summer, and subarctic summer standard atmospheres including two cloud layers described in the text.

this two cloud-layer case, this involved four calculations: one for clear-sky, one for each cloud separately, and one for both clouds together. These results were then combined according to partial cloud fraction. Clear layers separate the two cloud layers, so the clouds were treated with random cloud overlap. In each instance, the DISORT and 2-stream versions of RRTM produce similar heating rates and fluxes, though they differ in heating by as much as  $0.5 \text{ Kd}^{-1}$  in the high cloud in each atmosphere.

In contrast, the NCEP\_SW model produces excess heating within the low cloud by more the  $5 \text{ Kd}^{-1}$  (in addition to the deficient heating in the stratosphere). As a result, NCEP\_SW upward TOA fluxes and downward surface fluxes differ from the reference model by more the  $50 \text{ Wm}^{-2}$  for these cases.

## RRTM\_SW Comparison to ECMWF\_SW

Downward flux and heating rate profiles from the currently operational ECMWF six-band shortwave model also show considerable departures from RRTM\_SW. Figure 5 shows differences in downward flux and heating rate between RRTM\_SW and ECMWF\_SW for all of the Garand et al. (2001) profiles that have precipitable water amounts greater than 2 cm. Differences (RRTM-ECMWF) are plotted for each profile and are separated into categories of column water amount. The profile with the highest water amount (6.7 cm, plotted in black) produces a difference in downward surface flux of  $15 \text{ Wm}^{-2}$ .

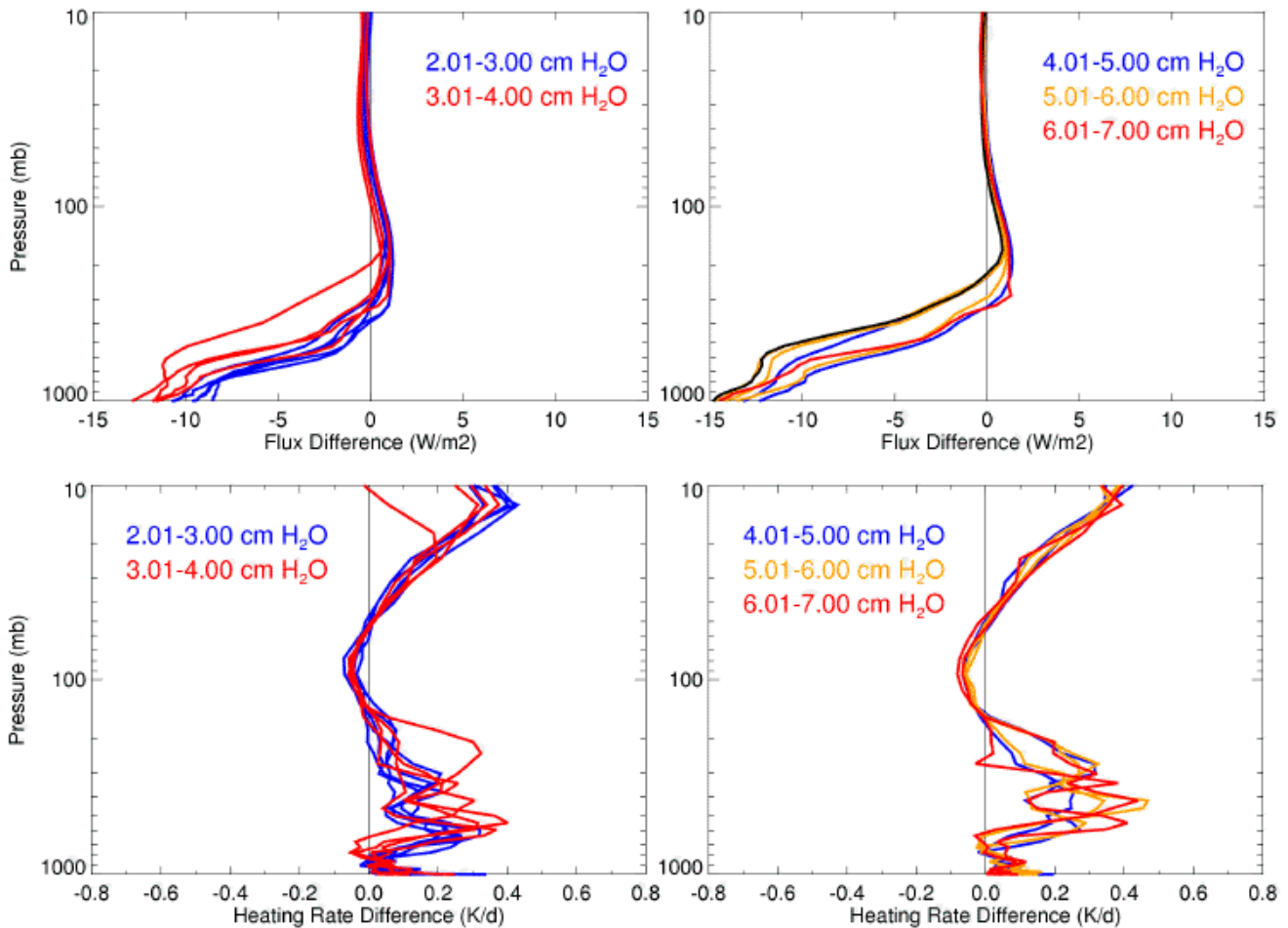


**Figure 5.** Differences between RRTM\_SW and the operational ECMWF shortwave model (RRTM-ECMWF), for all profiles of Garand et al. (2001) with precipitable water vapor greater than 2 cm, for downward flux (top panels) and heating rate (bottom panels). Plot color identifies the column water amount (cm) in the profile as shown in the legend.

Other high water profiles produce tropospheric heating rate differences as large as  $0.4 \text{ Kd}^{-1}$ . Profiles with less than 2 cm of precipitable water (not shown) produce smaller differences. An apparent dependence of the differences in downward surface flux on water amount suggests that the ECMWF\_SW model has too little water absorption in the troposphere. Closer analysis has shown that the differences are caused by combined (though offsetting) deficiencies in absorption from both dry gases and water vapor.

An adjustment to the ECMWF shortwave absorption has been developed and applied by AER to minimize the differences. These modifications include a quadratic adjustment that is applied to reduce the dry gas absorption as a function of pressure, while water vapor is scaled upward with a quadratic expression based on the column amount of water vapor. Figure 6 shows model differences in downward flux and heating rate after these modifications to the ECMWF\_SW model. Downward flux is increased in the modified ECMWF\_SW by as much as  $5 \text{ Wm}^{-2}$  by the dry gas adjustment and reduced as much as  $15\text{-}20 \text{ Wm}^{-2}$  by the water vapor scaling. Heating rate differences are also significantly reduced. This exercise illustrates the capability of utilizing RRTM\_SW or RRTMG\_SW as reference calculations for improving general circulation model radiative transfer.

## Summary

A separate version of RRTM\_SW\_V2.4 has been developed that uses a 2-stream algorithm for radiative transfer and scattering (in place of DISORT) as well as half the number of g-points for greatly improved computational performance. This accelerated version, RRTMG\_SW, is intended for application to general circulation models. RRTMG\_SW has been shown to calculate clear-sky fluxes at any level within  $2 \text{ Wm}^{-2}$  of RRTM\_SW and to calculate fluxes in the presence of low cloud within about  $8 \text{ Wm}^{-2}$ . RRTM\_SW itself compares very closely to the high-resolution, data-validated multiple scattering model, CHARTS.

RRTM\_SW has been used to evaluate downward flux biases in the ECMWF operational six-band shortwave model. These differences, due to water vapor, are as much as  $15\text{-}20 \text{ Wm}^{-2}$  in high water atmospheres. Heating rates differ by as much as  $0.4 \text{ Kd}^{-1}$ . Quadratic adjustments for both dry gas and water vapor absorption have been developed for ECMWF\_SW that significantly reduce these biases relative to RRTM\_SW.

RRTMG\_SW has been compared to the NCEP shortwave code currently operational in the GFS forecast model, and the later has been shown to have clear-sky biases in TOA upward flux and in downward surface flux and a significant cold bias in the heating rate profile in the troposphere and stratosphere. NCEP is currently evaluating the GFS shortwave model by extensive comparison to RRTM and is testing RRTMG\_SW for possible GFS implementation.

## Corresponding Author

Michael J. Iacono, [mike@aer.com](mailto:mike@aer.com), (781) 761-2208



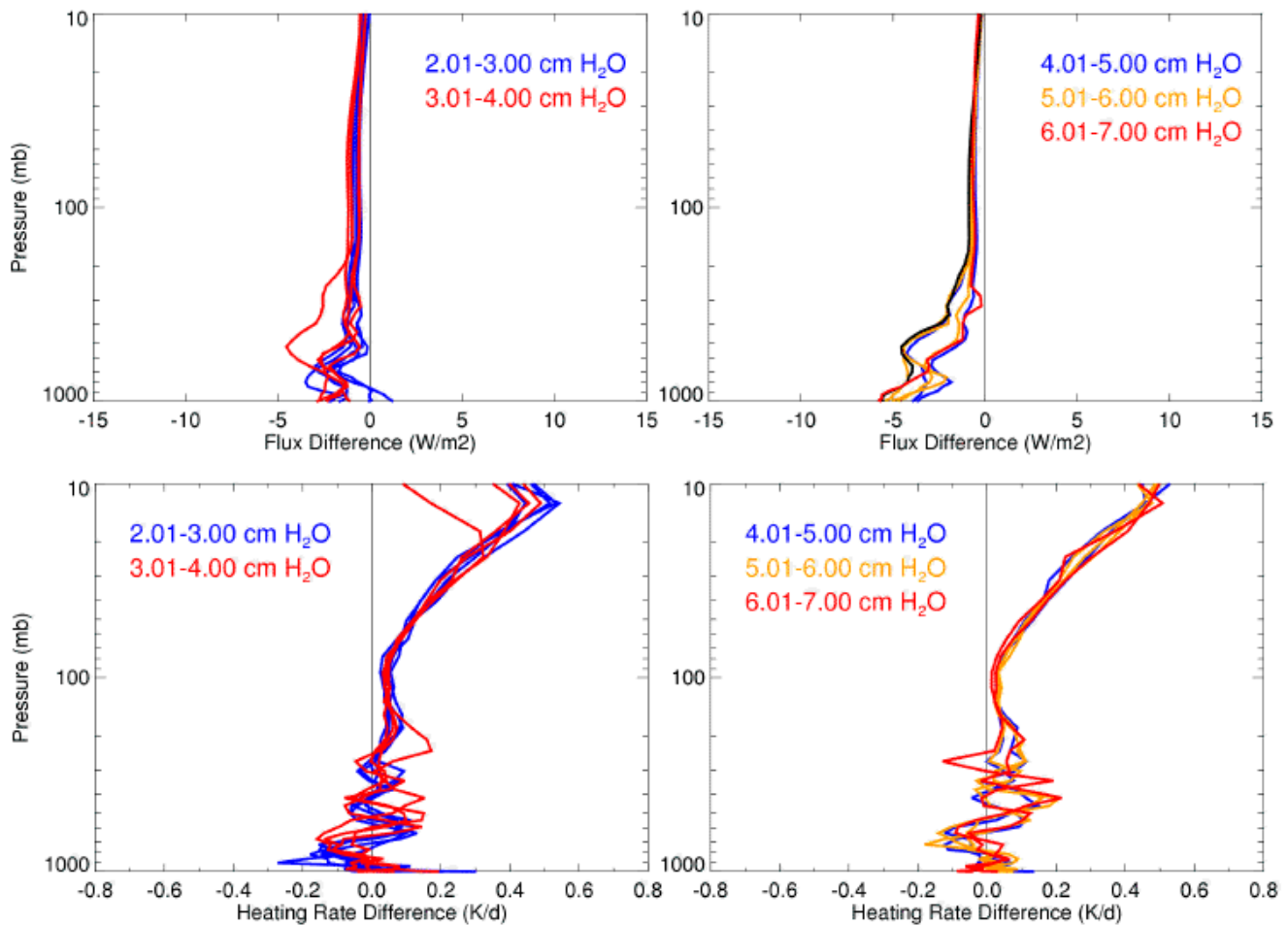


**Figure 6.** Differences between RRTM\_SW and the AER-modified ECMWF shortwave model (RRTM-ECMWF), for all profiles of Garand et al. (2001) with precipitable water vapor greater than 2 cm, for downward flux (top panels) and heating rate (bottom panels). Plot color identifies the column water amount (cm) in the profile as shown in the legend.

## References

Barker, H. W., and co-authors, 2003: Assessing 1-D atmospheric solar radiative transfer models: Interpretation and Handling of Unresolved Clouds. *J. Clim.*, **16**, 2676–2699.

Clough, S. A., M. W. Shephard, E. J. Mlawer, J. S. Delamere, M. J. Iacono, K. Cady-Pereira, S. Boukabara, and P. D. Brown, 2004: Atmospheric radiative transfer modeling: A Summary of the AER Codes. *J. Quant. Spectrosc. Radiat. Transfer*, in press.

Garand, L., and co-authors, 2001: Radiance and Jacobian intercomparison of radiative transfer models applied to HIRS and AMSU channels. *J. Geophys. Res.*, **106**, 24,017–24,031.

Hu, Y. X., and K. Stamnes, 1993: An accurate parameterization of the radiative properties of water clouds suitable for use in climate models. *J. Clim.*, **6**, 728–742.

Iacono, M. J., E. J. Mlawer, S. A. Clough, and J.-J. Morcrette, 2000: Impact of an improved longwave radiation model, RRTM, on the energy budget and thermodynamic properties of the NCAR community climate model, CCM3. *J. Geophys. Res.*, **105**, 14,873–14,890.

Iacono, M. J., J. S. Delamere, E. J. Mlawer, S. A. Clough, and J.-J. Morcrette, 2002: Cloudy sky RRTM shortwave radiative transfer and comparison to the revised ECMWF shortwave model. In *Proceedings of the Twelfth Atmospheric Radiation Measurement (ARM) Science Team Meeting*, ARM-CONF-2002. U.S. Department of Energy, Washington, D.C. Available URL: [http://www.arm.gov/publications/proceedings/conf12/extended\\_abs/iacono-mj.pdf](http://www.arm.gov/publications/proceedings/conf12/extended_abs/iacono-mj.pdf)

Moncet, J.-L., and S. A. Clough, 1997: Accelerated monochromatic radiative transfer for scattering atmospheres: Application of a New Model to Spectral Radiance Observations. *J. Geophys. Res.*, **102**, 21,853–21,866.